Distributed Power Control with Active Cell Protection in Future Cellular Systems

Zhe Ren*, Markus Jäger†, Sławomir Stańczak‡, Peter Fertl*
*BMW Group Research and Technology, Hanauerstrasse 46, Munich, Germany
†Munich University of Technology, Arcisstrasse 21, Munich, Germany
‡Fraunhofer Institute for Telecommunications Heinrich Hertz Institute, Einsteinufer 37, Berlin
{zhe.ren, peter.fertl}@bmw.de, markus.jaeger@tum.de, slawomir.stanczak@hhi.fraunhofer.de

***Abstract*—Distributed power control schemes have been intensively studied in the literature for uplink transmissions in cellular networks as well as in ad hoc networks. In these schemes, the signal to interference plus noise (SINR) requirements of the new users are gradually approached without violating the existing links. In this paper, we consider a downlink cellular scenario, in which new nomadic cells seek admission to the network. A distributed power control algorithm with active cell protection is presented, where a cell is said to be active if it has sufficient resources to support the connected users and, otherwise, it is said to be inactive. With the proposed algorithm, inactive cells lower their loads by gradually performing power ramping, while active cells scale their transmission power accordingly, to avoid being overloaded. We prove the active cell protection property and compare the convergence of the algorithm under different interference assumptions. Further, we present an algorithm for adapting the power ramping factor in power limited scenarios for further performance enhancements.**

I. Introduction

Distributed Power Control (DPC) is one of the fundamental mechanisms for resource allocation in wireless communication systems. DPC has been extensively studied in the context of single-carrier networks including the uplink channel and the distributed wireless mesh networks [1]–[7]. Based on a noiseless power control scheme in [1], the authors propose in [2] an iterative DPC algorithm that converges to the optimal power vector where a linear interference plus noise model is considered. The idea is further extended in [3] by adding Active Link Protection (ALP) such that the Quality of Service (QoS) for the users do not drop below the requirements during the transient phase. The energy-robustness trade-off of ALP/DPC is discussed in [4], where the authors propose an algorithm, denoted as the Robust Distributed Power Control (RDPC), to dynamically adjust the control parameter. Furthermore, the ALP/DPC framework has been extended in the context of Standard Interference Functions (SIFs) in [5], [6] and detailed analyses on the convergence performance and power limits are given in [5]. Another class of interference functions, proposed in [7] as General Interference Functions (GIFs), reflecting the case of zero noise interference, is also proven there to be a suitable interference function for the DPC/ALP model.

The abovementioned papers merely study cellular uplink transmissions or ad-hoc networks with focus on the Signal to Interference plus Noise Ratio (SINR) performance. Recently, the concept of 5G nomadic networks [8] raised new interest in downlink power control schemes for network-level QoS requirements. Nomadic networks, comprising randomly distributed nodes (e.g., parked vehicles with on-board relay node (RN) infrastructures), are regarded as an important 5G system component that allows for a flexible and dynamic network extension [9]. The locations of such RNs, referred to as nomadic RNs, are random and not controlled by the network operators. Moreover, the nomadic RNs operate in a self-organized fashion and are activated based on capacity, coverage or energy efficiency demands. Algorithms for the activation and deactivation of nomadic relays have been identified as the key techniques to enable such a dynamic network [10], [11]. An unavoidable issue is that the additional interference generated by the newly activated nomadic nodes might severely affect the neighboring active cells, such that the cells become overloaded. Hence, certain mechanisms are required to protect the active cells.

In this paper, we generalize the ALP algorithm of [5] in order to provide Active Cell Protection (ACP), where a cell, either a base station (BS) or a nomadic RN, is *active* if the cell is not overloaded and has sufficient resources for supporting the QoS of the connected nodes. Therefore, this paper extends the algorithm of [5] to relay-assisted cellular networks where multiple user equipments (UEs) are served by a single BS (transmitter). In other words, the algorithm of [5] is a special case of our algorithm, if there are no RNs and each BS serves only one UE. Moreover, we discuss the algorithm performance under different interference models: static interference model as in [12]–[14] and dynamic interference model as in [11], [15]. We prove the SIF property and hence the convergence of the proposed ACP algorithm under both assumptions. Furthermore, power constraints and signaling issues are also discussed for practical implementations. Simulations confirm that the proposed algorithm can be applied to nomadic networks which benefit significantly during the activation procedure. Note that due to the page limitation, we only sketch the proofs for the lemmas and propositions in this paper.

[1]Part of this work has been performed in the framework of the FP7 project ICT-317669 METIS, which is partly funded by the European Union. The authors would like to acknowledge the contributions of their colleagues in METIS, although the views expressed are those of the authors and do not necessarily represent the project.

The rest of the paper is organized as follows: Section II presents the system model. The load interference function is introduced in Section III, where some of its important properties are proven. In Section IV, the active cell protection algorithm is presented, while simulation and conclusion are provided in Section V and Section VI, respectively.

II. System Model

Based on the model in our previous work [10], we consider the downlink channel of a nomadic relay network with M BSs, N UEs and K RNs. The set of BSs, RNs and UEs are denoted by $\mathcal{B}$, $\mathcal{R}$ and $\mathcal{U}$, respectively. Furthermore, we use direct links, relay links and access links to denote the BS-UE, BS-RN and RN-UE links, respectively.[2] In this paper, we consider L3-RNs according to the Long Term Evolution (LTE) standard [16]. Such RNs are seen by the UEs as separate cells that have all the Radio Resource Management (RRM) functionalities of the BSs: the RNs are able to reuse the resources of the BS for the access link transmissions, while the relay links and direct links compete for resources allocated to the corresponding BS.

The amount of bandwidths (in Hz) at BSs and RNs are fixed and grouped in vectors $\mathbf{b}^{(\mathrm{m})} = (b_1^{(\mathrm{m})}, \ldots, b_M^{(\mathrm{m})})^T$ and $\mathbf{b}^{(\mathrm{k})} = (b_1^{(\mathrm{k})}, \ldots, b_K^{(\mathrm{k})})^T$, respectively. The vector of the required minimum rates (in bit/s) of the UEs is denoted by $\mathbf{r}^{(\mathrm{n})} = (r_1^{(\mathrm{n})}, \ldots, r_N^{(\mathrm{n})})^T$. Note that each UE can be connected either to an RN or directly to a BS (not to both simultaneously), while an RN can only be connected to a BS. The Spectral Efficiency (SE) of a link (i,j) is assumed to be (in bit/s/Hz)

$$\omega_{i,j} = \log(1 + \tau_{i,j}) \tag{1}$$

where $\tau_{i,j}$ denotes the corresponding SINR as defined in (2). Throughout the paper we take the following assumptions:

(A.1) The parameters $\mathbf{r}^{(\mathrm{n})}$, $\mathbf{b}^{(\mathrm{m})}$ and $\mathbf{b}^{(\mathrm{k})}$ are known parameters at a central network unit or can be estimated reliably.

(A.2) While access links and direct links interfere with each other, the RNs use separate time-frequency resources on the relay links and access links. Hence the access links do not interfere with the relay links.

(A.3) In the previous work [10], we considered the worst-case interference model in order to ensure the bandwidth constraints. In order to further optimize the network, we adapt a more realistic interference model. [15], [17], [18], where interference power is scaled by the load (denoted as ρ) of the interfering BSs.

As a result, the SINR of a link (i,j) is given by

$$\tau_{i,j} = \begin{cases} \frac{p_i g_{i,j}}{\sum_{d \in \mathcal{B}, d \neq i} p_d g_{d,j} \rho_d + \sigma_j} & \text{for } j \in \mathcal{R}, \\ \frac{p_i g_{i,j}}{\sum_{d \in \mathcal{B} \bigcup \mathcal{R}, d \neq i} p_d g_{d,j} \rho_d + \sigma_j} & \text{for } j \in \mathcal{U}. \end{cases} \tag{2}$$

Herein, σ_j, p_i and $g_{i,j}$ refer to the receiver-side noise power, transmission power and channel gain for link (i,j), respectively, while ρ_d denotes the load of the node d which is defined as the ratio of the amount of used bandwidth for supporting the QoS of the assigned UEs to the available bandwidth at the node. Note that $\rho_d = 1$, if we consider a static worst-case interference model as in many load balancing studies [12]–[14]. We explain the load function ρ in the Section II-A in more detail. Note that $\tau_{i,j} > 0$ always holds, since both received power and interference plus noise are positive values. Furthermore, a positive $\tau_{i,j}$ exists also for the case when both $i, j \in \mathcal{R}$, however, we do not allow a connection between RNs in this work.

A. Load Power Coupling Model

In this paper, we deal with the power control problem and assume the user assignment is already established. Further, we denote $\mathcal{U}_i$ and $\mathcal{R}_i$ to be the set of UEs and RNs that are connected to node i. We define $\boldsymbol{\rho} \triangleq [\begin{smallmatrix} \boldsymbol{\rho}_i^{(\mathrm{m})} \\ \boldsymbol{\rho}_i^{(\mathrm{k})} \end{smallmatrix}] = [\rho_1, \ldots \rho_M, \rho_{M+1}, \ldots, \rho_{M+K}]^T \in \mathbb{R}_+^{M+K}$, $i \in \mathcal{B} \bigcup \mathcal{R}$, to be the vector of loads at the BSs and RNs, where the i-th entry of the load vector can be calculated as

$$\begin{aligned} \rho_i &= \rho_i^{(1)} + \rho_i^{(2)}, \quad i \in \mathcal{B} \bigcup \mathcal{R} \\ &= \underbrace{\sum_{j \in \mathcal{U}_i} \frac{r_j^{(\mathrm{n})}}{b_i \omega_{i,j}(\boldsymbol{\rho})}}_{\text{direct/access links}} + \underbrace{\sum_{k \in \mathcal{R}_i} \frac{r_k^{(\mathrm{k})}}{b_i \omega_{i,k}(\boldsymbol{\rho})}}_{\text{relay links}} \\ &= \sum_{j \in \mathcal{U}_i} \frac{r_j^{(\mathrm{n})}}{b_i \omega_{i,j}(\boldsymbol{\rho})} + \sum_{k \in \mathcal{R}_i} \sum_{j \in \mathcal{U}_k} \frac{r_j^{(\mathrm{n})}}{b_i \omega_{i,k}(\boldsymbol{\rho})}. \end{aligned} \tag{3}$$

Herein, $\rho_i^{(1)}$ and $\rho_i^{(2)}$ refer to the load corresponding to the UEs (direct/access links) and RNs (relay links), respectively, while $r_j^{(\mathrm{k})}$ is the rate requirement of an RN, which is the sum rate of all the UEs connected to this RN:

$$r_k^{(\mathrm{k})} = \sum_{j \in \mathcal{U}_k} r_j^{(\mathrm{n})}, \quad \text{for } j \in \mathcal{U}, k \in \mathcal{R}\,. \tag{4}$$

Thus, for a given $\mathbf{p}$, the total load is determined by the function $\mathbf{F} = [F_1, \ldots, F_{M+K}] : \mathbb{R}^{2\times(M+K)} \to \mathbb{R}^{M+K}$ given by

$$\boldsymbol{\rho} = \mathbf{F}(\boldsymbol{\rho}, \mathbf{p}) = \mathbf{F}^{(1)}(\boldsymbol{\rho}, \mathbf{p}) + \mathbf{F}^{(2)}(\boldsymbol{\rho}, \mathbf{p}) \tag{5}$$

where $\rho_i^{(1)} = F_i^{(1)}(\boldsymbol{\rho}, \mathbf{p})$ and $\rho_i^{(2)} = F_i^{(2)}(\boldsymbol{\rho}, \mathbf{p})$ with $\mathbf{p} \triangleq [p_1, \ldots, p_{M+K}]^T$. We refer to the model in (5) as *dynamic interference* model, indicating that the load depends on itself via interference. If we consider the *static interference* model, for which we decouple the dependencies on the load vector of both sides in (5), we have:

$$\boldsymbol{\rho} = \mathbf{F}(\boldsymbol{\rho}', \mathbf{p}), \tag{6}$$

where $\boldsymbol{\rho}'$ is not related to $\boldsymbol{\rho}$ and determines the interference level. In particular, we get the *worst-case interference* model, if we set $\boldsymbol{\rho}' = \mathbf{1}$[3]. Note that in a real system, the load can not be larger than 1. Hence, we can write the real load as:

$$\bar{\boldsymbol{\rho}} = \min(\boldsymbol{\rho}, \mathbf{1}). \tag{7}$$

[2]Throughout this paper, notations with superscripts (m), (k) and (n) are variables associated with BSs, RNs and UEs, respectively, while notations with (m,n), (m,k) and (k,n) are referring to the direct links, relay links and access links, respectively.

[3]Throughout the paper, $\mathbf{1}^l(\mathbf{0}^l)$ refers to column vector of length l. If not specified, $\mathbf{1}(\mathbf{0})$ is a column vector with proper length for matrix operator. Furthermore, $\mathbf{1}^{m\times n}(\mathbf{0}^{m\times n})$ refers to an $m\times n$ matrix of ones(zeros). Further, the equalities and inequalities are performed element wise for vectors.

III. Load Interference Function

We define $\mathbf{I}(\mathbf{p}) = [I_1(\mathbf{p}), \ldots, I_{M+K}(\mathbf{p})] : \mathbb{R}_+^{M+K} \rightarrow \mathbb{R}_{++}^{M+K}$ to be the vector of the *Load Interference Functions*:[4]

$$I_i(\mathbf{p}) = \begin{cases} p_i F_i(\boldsymbol{\rho}, \mathbf{p}) & \text{for} \quad \mathbf{p} > \mathbf{0}, \\ \sum\limits_{j \in \mathcal{U}_i \bigcup \mathcal{R}_i} \sum\limits_{d \in \mathcal{I}_i} \frac{r_j (p_d g_{d,j} \rho_d + \sigma_j)}{b_i g_{i,j}} & \text{otherwise}, \end{cases} \tag{8}$$

where $\mathcal{I}_i$ refers to the set of interfering cells to cell i.

Lemma 1. $I_i(\mathbf{p})$ is a well defined *positive continuous* function: $\mathbb{R}_+^n \rightarrow \mathbb{R}_{++}$. Furthermore, if $I_i(\mathbf{p})$ is an SIF as in Definition 1 for $\mathbf{p} > \mathbf{0}$, it is also an SIF for $\mathbf{p} \geq \mathbf{0}$.

Proof (sketch): $I_i(\mathbf{p})$ is positive and continuous for $\mathbf{p} > \mathbf{0}$ by assuming the continuity of the load vector $\boldsymbol{\rho}$ with respect to $\mathbf{p}$ (details of proof omitted in this paper). Then, we follow L' Hospital's rule for $p_i = 0$:

$$\begin{aligned} \lim_{p_i \rightarrow 0^+} I_i(\mathbf{p}) &= \lim_{p_i \rightarrow 0^+} \sum_{j \in \mathcal{U}_i \bigcup \mathcal{R}_i} \frac{r_j (1 + \frac{g_{i,j} p_i}{\sum_{d \in \mathcal{I}_i} p_d g_{d,j} \rho_d + \sigma_j})}{b_i \frac{g_{i,j}}{(\sum_{d \in \mathcal{I}_i} p_d g_{d,j} \rho_d + \sigma_j)}} \\ &= I_i(\mathbf{p})|_{p_i = 0} > 0. \end{aligned}$$

Thus, $I_i(\mathbf{p})$ is a positive continuous function for $\mathbf{p} \geq \mathbf{0}$. Moreover, it can be justified due to continuity that, if the two properties of the SIF defined as in Definition 1 hold for $\mathbf{p} > \mathbf{0}$, they also hold for $\mathbf{p} \geq \mathbf{0}$. ∎

Hence, in order to prove that $\mathbf{I}(\mathbf{p})$ is a vector of SIF functions for all $\mathbf{p} \geq \mathbf{0}$, it is sufficient to prove that $I_i(\mathbf{p})$ satisfies the two properties for $\mathbf{p} > \mathbf{0}$.

Definition 1 (SIF [6])**.** Let $\mathbf{z} \in \mathbb{R}_+^n$ for arbitrary $n \geq 1$. A positive function $f : \mathbb{R}_+^n \rightarrow \mathbb{R}_{++}$ is an SIF if:

- Scalability: $\forall_{\mathbf{z} \geq 0} \forall_{\alpha > 1}$, $\alpha f(\mathbf{z}) > f(\alpha \mathbf{z})$,
- Monotonicity: if $\mathbf{z} \geq \mathbf{z}' \geq 0$, then $f(\mathbf{z}) \geq f(\mathbf{z}')$.

In the following, we prove that the load interference function is SIF for all $\mathbf{p} > \mathbf{0}$ under both the *static* and the *dynamic interference* assumption. Note that (6) is used to compute $\boldsymbol{\rho}$ in (8) for the static interference model while (5) is applied to the dynamic interference model. First, we formulate a sufficient condition for the monotonicity property:

Lemma 2. Let $\mathbf{z} \in \mathbb{R}_+^n$ for arbitrary $n \geq 1$. The monotonicity property is fulfilled if $f : \mathbb{R}_+^n \rightarrow \mathbb{R}_{++}$ is continuously differentiable over $\mathbf{z} \in \mathbb{R}_{++}^n$ with only non-negative gradients: $\nabla f(\mathbf{z}) \geq \mathbf{0}$ for all $\mathbf{z} \in \mathbb{R}_{++}^n$.

Proof (sketch): Let $\mathbf{x}, \mathbf{z} \in \mathbb{R}_{++}^n$ be arbitrary and, without loss of generality, assume that $\mathbf{x} \leq \mathbf{z}$. Now let $\mathbf{y}^{(i)} = (0, \ldots, 0, z_i - x_i, 0, \ldots, 0)$, $1 \leq i \leq n$, is a vector with zeros everywhere except for the i-th position which is equal to $z_i - x_i$. Since $\nabla f(\mathbf{z}) \geq \mathbf{0}$ for all $\mathbf{z} \in \mathbb{R}_{++}^n$, we have $f(\mathbf{x}) \leq f(\mathbf{x} + \mathbf{y}^{(1)}) \leq f(\mathbf{z} + \mathbf{y}^{(1)} + \mathbf{y}^{(2)}) \leq \cdots \leq f(\mathbf{x} + \sum_{i=1,\ldots,n} \mathbf{y}^{(i)}) = f(\mathbf{z})$ ∎

Proposition 1. $\mathbf{I}(\mathbf{p})$ is an SIF assuming static interference.

[4]Throughout this paper, the inequalities are all element wise comparisons.

Proof (sketch): According to (6), we have the analytical form of (8) under the static interference model by inserting a constant load vector. Since r_j, b_i and $g_{i,j}$ are all positive constants, it suffices to prove that $\tilde{I}_i(\mathbf{p}) = p_i / \log(1 + \frac{p_i}{\sum_{d \in \mathcal{I}_i} p_d + \sigma_j})$ satisfies Definition 1.

For scalability, It can verified that $\partial \tilde{I}_i(\mathbf{p}) / \partial \sigma_j > 0$. Thus,

$$\begin{aligned} \tilde{I}_i(\alpha \mathbf{p}) &= \frac{\alpha p_i}{\log(1 + \frac{p_i}{\sum_{d \in \mathcal{I}_i} p_d + \sigma_j / \alpha})} \\ &< \frac{\alpha p_i}{\log(1 + \frac{p_i}{\sum_{d \in \mathcal{I}_i} p_d + \sigma_j})} = \alpha \tilde{I}_i(\mathbf{p}). \end{aligned}$$

For monotonicity, we show that Lemma 2 is satisfied since the gradient of $\tilde{I}_i(\mathbf{p})$ is non-negative for all $\mathbf{p} > \mathbf{0}$. Details of the proof are omitted due to the space limitation. ∎

Lemma 3. There exists an explicit function $\boldsymbol{\rho} = \mathbf{G}(\mathbf{p}) : \mathbb{R}_+^{M+K} \rightarrow \mathbb{R}_+^{M+K}$ that takes power vector $\mathbf{p}$ as argument. Furthermore, if $\alpha \geq 1$, $\mathbf{G}(\alpha \mathbf{p}) < \mathbf{G}(\mathbf{p})$ element wise.

Proof (sketch): In [11, Prop.1], we have proven that there exists an explicit function that takes the assignments as input argument. Similarly, the existence of $\boldsymbol{\rho} = \mathbf{G}(\mathbf{p})$ with power vector as input can be proven. Without loss of generality, we assume the same noise power in the network. Then, we extend load functions $\mathbf{G}(\mathbf{p})$ and $\mathbf{F}(\boldsymbol{\rho}, \mathbf{p})$ as functions of both power $\mathbf{p}$ and noise σ, such that $\boldsymbol{\rho} = \mathbf{G}(\mathbf{p}, \sigma)$ and $\mathbf{F}(\boldsymbol{\rho}, \mathbf{p}) = \mathbf{F}(\boldsymbol{\rho}, \mathbf{p}, \sigma)$. Further, we define the implicit function

$$\tilde{\mathbf{F}}(\boldsymbol{\rho}, \mathbf{p}, \sigma) \triangleq \boldsymbol{\rho} - \mathbf{F}(\boldsymbol{\rho}, \mathbf{p}, \sigma). \tag{9}$$

According to the implicit function theorem,[5]

$$\mathbf{J}_{\mathbf{G}}^{\sigma}(\boldsymbol{\rho}, \mathbf{p}, \sigma) = -\mathbf{J}_{\tilde{\mathbf{F}}}^{\boldsymbol{\rho}}(\boldsymbol{\rho}, \mathbf{p}, \sigma)^{-1} \mathbf{J}_{\tilde{\mathbf{F}}}^{\sigma}(\boldsymbol{\rho}, \mathbf{p}, \sigma). \tag{10}$$

According to [11, Prop.2], the inverse of $\mathbf{J}_{\tilde{\mathbf{F}}}^{\boldsymbol{\rho}}(\boldsymbol{\rho}, \mathbf{p}, \sigma)$ exists with only non-negative elements. Moreover, it can be easily verified that $\partial \mathbf{F}_i / \partial \sigma$ is positive and $\partial \tilde{\mathbf{F}}_i / \partial \sigma$ (which is the i-th entry in $\mathbf{J}_{\tilde{\mathbf{F}}}^{\sigma}(\boldsymbol{\rho}, \mathbf{p}, \sigma)$) is negative. Thus, $\mathbf{J}_{\mathbf{G}}^{\sigma}(\boldsymbol{\rho}, \mathbf{p}, \sigma) > \mathbf{0}$ for $\sigma > 0$, indicating a monotonically increasing property on σ. Therefore, for $\alpha > 1$, $\mathbf{G}(\alpha \mathbf{p}, \sigma) = \mathbf{G}(\mathbf{p}, \sigma / \alpha) < \mathbf{G}(\mathbf{p}, \sigma)$. ∎

Proposition 2. $\mathbf{I}(\mathbf{p})$ is an SIF assuming dynamic interference.

Proof (sketch): For $p_i > 0$ we can rewrite the load interference function as $I_i(\mathbf{p}) = p_i \mathbf{G}_i(\mathbf{p})$ according to Lemma 3.

For scalability, if $\alpha > 1$, using Lemma 3 we have easily $I_i(\alpha \mathbf{p}) = \alpha p_i \mathbf{G}(\alpha \mathbf{p}) < \alpha p_i \mathbf{G}(\mathbf{p}) = \alpha I_i(\mathbf{p})$.

For monotonicity, we use the implicit function defined in (9) and calculate the Jacobian with respect to $\mathbf{p}$ as

$$\mathbf{J}_{\mathbf{G}}^{\mathbf{p}}(\boldsymbol{\rho}, \mathbf{p}, \sigma) = -\mathbf{J}_{\tilde{\mathbf{F}}}^{\boldsymbol{\rho}}(\boldsymbol{\rho}, \mathbf{p}, \sigma)^{-1} \mathbf{J}_{\tilde{\mathbf{F}}}^{\mathbf{p}}(\boldsymbol{\rho}, \mathbf{p}, \sigma). \tag{11}$$

Following the proof in Lemma 3: we know from [11, Prop.2] that $\mathbf{J}_{\tilde{\mathbf{F}}}^{\boldsymbol{\rho}}(\boldsymbol{\rho}, \mathbf{p}, \sigma)^{-1}$ is non-negative and $\mathbf{J}_{\tilde{\mathbf{F}}}^{\mathbf{p}}(\boldsymbol{\rho}, \mathbf{p}, \sigma)$ is non-positive. Therefore, $\mathbf{J}_{\mathbf{G}}^{\mathbf{p}}(\boldsymbol{\rho}, \mathbf{p}, \sigma)$ exists as a matrix with only non-negative elements for all $\mathbf{p} > 0$. Thus, $\partial I_i(\mathbf{p}) / \partial p_j = \mathbf{G}_i(\mathbf{p}) \frac{\partial p_i}{\partial p_j} + p_i \frac{\partial \mathbf{G}_i}{\partial p_j} \geq 0$ which yields monotonicity of $I_i(\mathbf{p})$ according to Lemma 2. ∎

[5]Throughout this paper, we denote $\mathbf{J}_{\mathbf{F}}^{\mathbf{x}}(\cdot)$ as the Jacobien of function $\mathbf{F}(\cdot)$ with respect to $\mathbf{x}$. Furthermore, the i-th row and the an entry i, j in $\mathbf{J}_{\mathbf{F}}^{\mathbf{x}}(\cdot)$ are denoted as $\mathbf{J}_{\mathbf{F}_i}^{\mathbf{x}}(\cdot)$ and $\mathbf{J}_{\mathbf{F}_i}^{\mathbf{x}_j}(\cdot)$, respectively

IV. Distributed Power Control

With the load interference function in hand, we proceed along similar lines as [3], [5] and formulate the distributed power control algorithm with active cell protection as follows:

$$p_i(\mathrm{t}+1) = \begin{cases} \delta I_i(\mathbf{p}(\mathrm{t})) & \text{for} \quad i \in \mathcal{A}_t, \\ \delta p_i(\mathrm{t}) = \delta^{(\mathrm{t}+1)} p_i(0) & \text{for} \quad i \in \mathcal{D}_t, \end{cases} \tag{12}$$

where we denote the active ($\rho_i \leq 1$) and inactive ($\rho_i > 1$) sets of cells at time instance t as $\mathcal{A}_\mathrm{t}$ and $\mathcal{D}_\mathrm{t}$, respectively. If $\mathbf{p}_i > \mathbf{0}$, this can be written in a more compact way as

$$p_i(\mathrm{t}+1) = \delta p_i(\mathrm{t}) \bar{\rho}_i(\mathbf{p}(\mathrm{t})), \tag{13}$$

where $\bar{\rho}_i$ is the real load as defined in (7). The algorithm can be understood as first scaling transmission power by the real load and then multiplying with a power incremental δ.

Remark 1. The proposed algorithm becomes the ALP algorithm in [5], if only one UE is associated with each BS. In this case, cell i is active if: $\frac{r_j}{b_i \log(1+\tau_{i,j})} \leq 1$, which is equivalent to the SINR threshold: $\tau_{i,j} \geq e^{r_j/b_i} - 1$.

Remark 2. In the previous works [3], [5], [6], the ALP property is considered only for $\delta > 1$. In this paper, the ALP/ACP is also valid for $\delta = 1$, however, indicating a power reduction control scheme. The proof is simple: For $\delta = 1$ and $\bar{\boldsymbol{\rho}} \leq \mathbf{1}$ we have $\mathbf{p}(\mathrm{t}+1) \leq \mathbf{p}(\mathrm{t})$ and hence, due to monotonicity, $\mathbf{I}(\mathbf{p}(\mathrm{t}+1)) \leq \mathbf{I}(\mathbf{p}(\mathrm{t}))$. Then, [5, Prop.2 and 3] proves the ACP.

Remark 3. Since $\mathbf{I}(\mathbf{p})$ is a vector of SIFs, all properties of the power control scheme in [5] hold also here for the algorithm in (12) or (13).

A. Admissibility and Convergence

The system is feasible, if there exists $\mathbf{p} \in \mathcal{P}$ with $\mathcal{P}$ denoting the feasible power region of the system, such that:

$$\mathbf{0} \leq \boldsymbol{\rho} \leq \mathbf{1}. \tag{14}$$

Similarly to [5], we distinguish three different cases for the feasibility of a full admission. Firstly, we consider the unlimited case, i.e., $\mathcal{P} = \mathbb{R}_+^{M+K}$.

(C.1) Fully admissible: there exists $\mathbf{p} \in \mathcal{P}$ such that $\mathbf{0} \leq \mathbf{F}(\mathbf{1}, \mathbf{p}) \leq \mathbf{1}/\delta$ or $\mathbf{0} \leq \mathbf{G}(\mathbf{p}) \leq \mathbf{1}/\delta$;

(C.2) δ-incompatible: (C.1) is not feasible but there exists $\mathbf{p} \in \mathcal{P}$ such that $\mathbf{0} \leq \mathbf{F}(\mathbf{1}, \mathbf{p}) \leq \mathbf{1}$ or $\mathbf{0} \leq \mathbf{G}(\mathbf{p}) \leq \mathbf{1}$;

(C.3) Not fully admissible: (C.1) and (C.2) are not feasible.

Note that for the worst-case interference model $\mathbf{F}(\mathbf{1}, \mathbf{p})$ applies, while $\mathbf{G}(\mathbf{p})$ is used for the dynamic interference system.

Proposition 3. In case of (C.1), for every cell i, $\lim_{t\to\infty} \rho_i = 1/\delta$ and $\lim_{t\to\infty} p_i < \infty$; In case of (C.2), for every cell i, $1/\delta < \lim_{t\to\infty} \rho_i < 1$ and $p_i \to \infty$; In case of (C.3),for $i \in \mathcal{A}_t$, $\lim_{t\to\infty} \rho_i = 1$, whereas $\lim_{t\to\infty} \rho_i > 1$ for $i \in \mathcal{D}_t$. Further, for all i, $p_i \to \infty$.

Proof (sketch): It follows directly [5, Prop. 4-6]. ∎

Now that there are two different interference models, we point out the performance differences of the two models with respect to admissibility and convergence.

Proposition 4. If (C.1) holds for worst-case interference, it also holds for dynamic interference assumption. If (C.2) holds for worst-case interference, (C.1) or (C.2) holds for dynamic interference assumption.

Proof (sketch): If (C.1) holds for worst-case model, there exists $\mathbf{p}^{(1)}$ such that $\mathbf{G}(\mathbf{p}^{(1)}) = \mathbf{F}(\mathbf{G}(\mathbf{p}^{(1)}), \mathbf{p}^{(1)}) \leq \mathbf{F}(\mathbf{1}, \mathbf{p}^{(1)}) \leq \mathbf{1}/\delta$; if (C.1) or (C.2) holds for worst-case model, there exists $\mathbf{p}^{(2)}$ satisfying $\mathbf{G}(\mathbf{p}^{(2)}) = \mathbf{F}(\mathbf{G}(\mathbf{p}^{(2)}), \mathbf{p}^{(2)}) \leq \mathbf{F}(\mathbf{1}, \mathbf{p}^{(2)}) \leq \mathbf{1}$. ∎

Proposition 5. If the system is admissible for dynamic interference (i.e., (C.1) or (C.2)), it is also admissible for the worst-case interference model.

Proof (sketch): If (C1) or (C2) holds for dynamic interference, there exists $\mathbf{p}^{(1)}$, such that $\mathbf{0} \leq \mathbf{G}(\mathbf{p}^{(1)}) \leq \mathbf{1}$. Applying $\delta = 1$ and using Proposition 3, the system converges to the power vector $\mathbf{p}^{(2)} < \infty$ such that $\mathbf{G}(\mathbf{p}^{(2)}) = \mathbf{1}$. Hence $\mathbf{G}(\mathbf{p}^{(2)}) = \mathbf{F}(\mathbf{1}, \mathbf{p}^{(2)}) = \mathbf{1}$ and the system is admissible also for worst-case interference models with $\mathbf{p}^{(2)}$. ∎

Proposition 4 and Proposition 5 indicate that the two interference models differ only when it is (C.2) for the worst-case model and (C.1) for the dynamic interference model. This difference vanishes as the power incremental δ goes to 1, indicating the equivalence of (C.1) and (C.2).

B. Power Constraints and Implementation

In practical systems, the transmission powers are limited. To take the power limit into account for (C.1)-(C.3), we denote the power limit by $\hat{\mathbf{p}} \in \mathbb{R}_+^{M+K}$ and denote $\mathcal{P} = \{\mathbf{p} | \mathbf{0} \leq \mathbf{p} \leq \hat{\mathbf{p}}\}$. In this paragraph, we still refer to (C.1)-(C.3) as the three levels of admissibility but under power constraints. It has been pointed out in [5] that full admission can not be guaranteed for (C.2) in power constrained cases since it requires infinite power for convergence. This requires a *smaller* δ to avoid (C.2) in a limited power scenario. In particular, from Proposition 4 and Proposition 5, we know that (C.2) happens more frequently under the worst-case interference model. On the other hand, in [4], it is well understood that larger δ trades-off convergence speed with energy consumption. In this work, energy consumption is not the optimization objective. Hence, we can optimize the convergence speed of the algorithm by using *large* values of δ as long as the power constraint is not violated. Based on all these observations, we propose an algorithm that dynamically controls δ as

$$p_i(\mathrm{t}+1) = \delta(t) p_i(\mathrm{t}) \bar{\rho}_i(\mathbf{p}(\mathrm{t})), \tag{15}$$

where positive initial powers, i.e. $\mathbf{0} < \mathbf{p}(0) \leq \hat{\mathbf{p}}$ and

$$\delta(\mathrm{t}) = \min_i \frac{\hat{p}_i}{p_i(\mathrm{t}) \bar{\rho}_i(\mathrm{t})}, \quad \text{for } i \in \mathcal{B} \bigcup \mathcal{R}. \tag{16}$$

Remark 4. Suppose the system power is bounded by $\mathbf{0} \leq \mathbf{p} \leq \hat{\mathbf{p}}$. First, $p_k(\mathrm{t}+1) = \min_i \frac{\hat{p}_i}{p_i(\mathrm{t}) \bar{\rho}_i(\mathrm{t})} p_k(\mathrm{t}) \bar{\rho}_k(\mathbf{p}(\mathrm{t})) \leq \frac{\hat{p}_k p_k(\mathrm{t}) \bar{\rho}_k(\mathbf{p}(\mathrm{t}))}{p_k(\mathrm{t}) \bar{\rho}_k(\mathrm{t})} = \hat{p}_k$. Then, the algorithm in (16) chooses the largest $\delta(t)$ at time t. This can be proven by formulating the feasible set of $\delta(\mathrm{t})$ which is $\bigcap_{i \in \mathcal{B} \bigcup \mathcal{R}} \{\delta | 1 \leq \delta \leq \frac{\hat{p}_i}{p_i(\mathrm{t}) \bar{\rho}_i(\mathrm{t})}\}$.

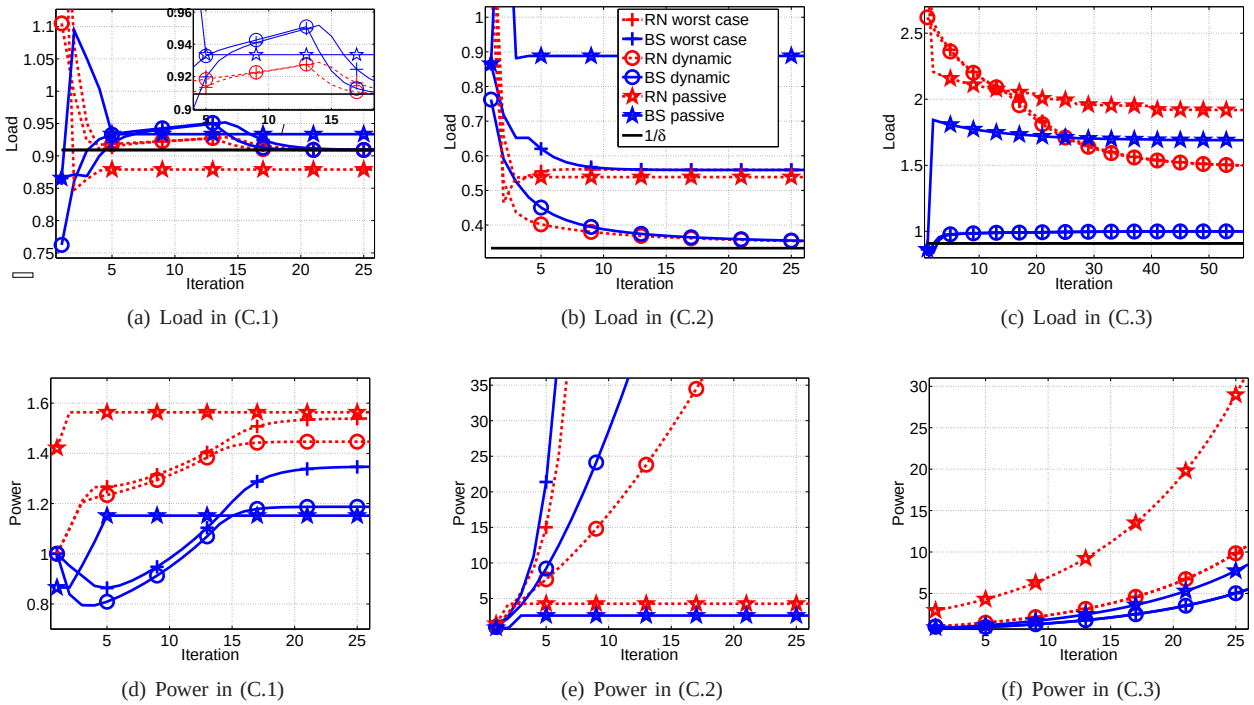

(a) Load in (C.1) (b) Load in (C.2) (c) Load in (C.3)

(d) Power in (C.1) (e) Power in (C.2) (f) Power in (C.3)

Fig. 1. Load and power performance in (C.1), (C.2), and (C.3)

Choosing the largest $\delta(\mathrm{t})$ leads to best robustness and speed of convergence according to the trade-off study in [4] to. Moreover, $\delta(\mathrm{t}) = \min_i \frac{\hat{p}_i}{p_i(\mathrm{t})\bar{\rho}_i(\mathrm{t})} \leq \frac{\hat{p}_k}{p_k(\mathrm{t})\bar{\rho}_k(\mathrm{t})} = \frac{\hat{p}_k}{p_k(\mathrm{t})}$, for $k \in \mathcal{D}_t$. As long as $\delta(\mathrm{t}) > 1$, $p_k(\mathrm{t})$ will increase until reaching the power bound $\hat{p}_k$ and $\delta(\mathrm{t})$ goes to 1. This means, as long as a cell stays inactive, $\delta(\mathrm{t})$ converges to 1. Thus, if the system is not (C.3), the algorithm in (15) ensures full admission.

The algorithm (13) or (15) is easy to implement in real systems, since both current power $p_i(t)$ and current load $\rho_i(t)$ are known or can be easily estimated at the cell i. For instance, in LTE, the UEs are able to measure the Reference Signal Received Power (RSRP), which is $p_i g_{i,j}$, and Reference Signal Received Quality (RSRQ), which can be seen as $\sum_{d\in\mathcal{I}_i} p_d g_{d,j} + \sigma_j$. These can be fed back to the cells such that ρ_i can be computed and the power control algorithm can be carried out. One critical point for implementation is that the value of δ should be synchronized among all cells. Especially, dynamical updating of δ requires to exchange information between the BSs.

V. Performance Evaluation

A nomadic relay network with 7 hexagon layout BSs, 50 randomly distributed RNs and 50 UEs is simulated. The other system parameters are listed in Table I. A simple cell and relay selection scheme is applied, where all UEs are either connected to the BS or UE with the best RSRP. An RN is seeking admission into the network with a certain rate QoS. We compare our ACP algorithm with an intuitive algorithm (Passive) : Active cells remain at the same power, whereas inactive cells iteratively increase their transmission powers.

$$p_i(\mathrm{t}+1) = \begin{cases} p_i(\mathrm{t}) & \text{for} \quad i \in \mathcal{A}_t, \\ \delta p_i(\mathrm{t}) = \delta^{(\mathrm{t}+1)} p_i(0), & \text{for} \quad i \in \mathcal{D}_t. \end{cases} \tag{17}$$

The weakness of the passive algorithm is that the active cells can become inactive as the interfering power from the inactive cells become critical.

The simulation results on the behavior of load and power are shown in Fig 1 for a power unlimited scenario. We choose to show the power and load performance of two representative cells: a nomadic RN that seeks for admission and a BS that is severely interfered by the RN. It can been seen that the RN is iteratively joining the network until the loads converge in all three cases. However, load violations can be observed within the first iterations using the passive algorithm (marked with stars), whereas the proposed algorithm ensures ACP in both interference assumptions (marked with circles and diamonds). Proposition 3 can be justified by examining the load and power performance for each (C.1), (C.2) and (C.3) in Fig 1. Furthermore, it is worth noting that a lower power convergence value is expected for the dynamic interference model than that for the worst-case model.

TABLE I
SIMULATION CONFIGURATIONS

Transmission Parameters	
initial transmission power	46 dBm for BS & 30 dBm for RN
available bandwidth	10 MHz for BS & 10 MHz for RN
antenna configuration	2 antennas for BSs, RNs and UEs
Channel and Noise Parameters in [dB]	
path loss model for all links	as in Table A.2.1.1.2-3 in [19]
noise figure	5 dB at UE & RN

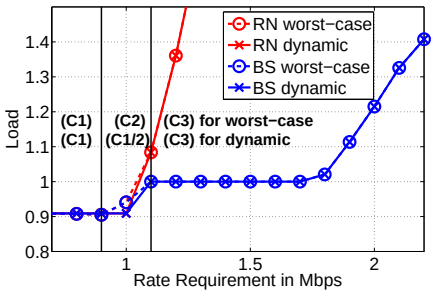

Fig. 2. Comparison of worst-case and dynamic interference model

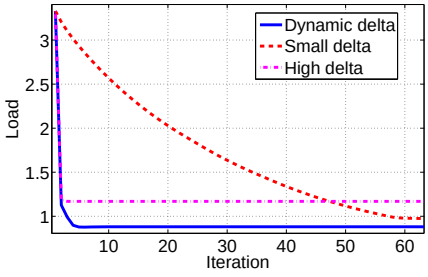

Fig. 3. Load behavior of various settings of δ

Fig 2 illustrates the comparison of load behavior between the worst-case and dynamic load assumption when the average rate requirement is steadily increased. The two horizontal lines separate the cases in which the system ends up with under a certain average rate requirement. For instance, the system is full admissible under both static and dynamic interference for rate requirements lower than 0.9 Mbps. By further increasing the rate requirement, the system under the worst-case interference model turns to be (C.2) whereas it is either (C.1) or (C.2) for the dynamic interference model. This can be observed by the different load convergence values for rate requirements between 0.9 Mbps and 1.1 Mbps, since according to Proposition 3, the two models have the same load convergence in (C.1), but different load convergences in (C.2). Furthermore, both scenarios are not fully admissible for rates equal or greater than 1.1 Mbps, since the loads converge to a value that is larger than 1.

Finally, we compare the ACP algorithm in (15)-(16) with a fixed delta algorithm in a power constrained scenario such that $p_i(t+1) = \min\{p_i(t+1), \hat{p}_i\}$. Fig 3 shows the importance of choosing a suitable δ: A high δ is preferable for fast convergence but can lead to (C.3). In contrast, a small δ implies a slow convergence speed. The proposed varying δ algorithm guarantees admission and achieves a high speed of convergence.

VI. Conclusion

In this paper, a distributed power control algorithm with active cell protection has been presented with the help of the SIF property. We have proven the active cell protection property of the algorithm and compared the convergence under different interference assumptions. With the proposed algorithm, the inactive cells can be gradually admitted into the network without violating the other active cells. We have also discussed the scenarios with limited powers and proposed an algorithm that iteratively adjusts the power incremental for performance enhancement. Simulation results have confirmed that the algorithm can be applied to the activation procedures of nomadic cells to protect the active cells.

References

[1] J. Zander, "Performance of Optimum Transmitter Power Control in Cellular Radio Systems," *IEEE Trans. Veh. Technol.*, vol. 41, pp. 57–62, Feb. 1992.

[2] G. J. Foschini and Z. Miljanic, "A Simple Distributed Autonomous Power Control Algorithm and its Convergence," *IEEE Trans. Veh. Technol.*, vol. 42, no. 4, pp. 641–646, Nov. 1993.

[3] N. Bambos, S. Chen, and G. Pottie, "Channel Access Algorithms with Active Link Protection for Wireless Communication Networks with Power Control," *IEEE/ACM Trans. Networking*, vol. 8, no. 5, pp. 583–597, 2000.

[4] C. W. Tan, D. P. Palomar, and M. Chiang, "EnergyRobustness Tradeoff in Cellular Network Power Control," *IEEE/ACM Trans. Networking.*, vol. 17, no. 3, pp. 912–925, Jun. 2009.

[5] S. Stanczak, M. Kaliszan, and N. Bambos, "Decentralized Admission Control for Power-Controlled Wireless Links," *Preprint available at http://arxiv.org/abs/0907.2896*, 2010.

[6] R. D. Yates, "A Framework for Uplink Power Control in Cellular Radio Systems," *IEEE J. Sel. Areas Communi.*, vol. 13, no. 7, pp. 1341–1347, 1995.

[7] H. Boche1 and M. Schubert, "Characterization of the Structure of General Interference Functions," in *International Symposia on Information Theory (ISIT), Nice, France*, June 2007.

[8] P. Popovski, V. Braun, H. P. Mayer, P. Fertl *et al.*, "ICT-317669-METIS/D1.1 Scenarios, requirements and KPIs for 5G mobile and wireless systems," EU-Project METIS (ICT-317669), Deliverable, 2013.

[9] P. Popovski, V. Braun, G. Mange, P. Fertl *et al.*, "ICT-317669-METIS/D6.2 Initial report on horizontal topics, first results and 5G system concept," EU-Project METIS (ICT-317669), Deliverable, 2014.

[10] Z. Ren, S. Stańczak, P. Fertl, and F. Penna, "Energy-Aware Activation of Nomadic Relays for Performance Enhancement in Cellular Networks," in *Proceedings of IEEE International Conference on Communications (ICC), Sydney, Australia, June, 2014*, pp. 1–6.

[11] Z. Ren, S. Stańczak, and P. Fertl, "Activation of Nomadic Relays in Dynamic Interference Environment for Energy Savings," in *Proceedings of IEEE Global Conference on Communications (GLOBECOM), Austin, Texas, Dec., 2014*, pp. 1–6.

[12] S. C. K. Son and G. de Veciana, "Dynamic Association for Load Balancing and Interference Avoidance in Multi-Cell Networks," *IEEE Trans. Wireless Commun.*, vol. 8, no. 5, p. 35663576, 2009.

[13] E. Pollakis, R. L. G. Cavalcante, and S. Stanczak, "Base Station Selection for Energy Efficient Network Operation with the Majorization-Minimization Algorithm," in *IEEE 13th International Workshop on Signal Processing Advances in Wireless Communications (SPAWC), Cesme, Turkey, June, 2012*, pp. 1–6.

[14] X. W. A. Sang, M. Madihian and R. D. Gitlin, "Coordinated Load Balancing, Handoff/Cell-site Selection, and Scheduling in Multi-Cell Packet Data Systems," *Proc. ACM MobiCom*, pp. 302–314, 2004.

[15] A. Fehske, H. Klessig, J. Voigt, and G. Fettwei, "Concurrent Load-Aware Adjustment of User Association and Antenna Tilts in Self-Organizing Radio Networks," *IEEE Trans. Veh. Technol.*, vol. 62, no. 5, pp. 1974–1988, 2013.

[16] 3GPP, *Evolved Universal Terrestrial Radio Access (E-UTRA); Physical layer for relaying operation*, 3GPP Std. 36.216 v10.3.1, 2011.

[17] I. Siomina and D. Yuan, "Analysis of Cell Load Coupling for LTE Network Planning and Optimization," *IEEE Trans. Wireless Commun.*, vol. 11, no. 6, pp. 2287–2297, 2012.

[18] R. L. G. Cavalcante, S. Stanczak, M. Schubert, A. Aisenblätter, and U. Türke, "Toward Energy-efficient 5G Wireless Communication Technologies," *IEEE Signal Processing Mag.*, 2014, to appear (see also http://arxiv.org/abs/1407.0344).

[19] 3GPP, *Evolved Universal Terrestrial Radio Access (E-UTRA); Further advancements for E-UTRA physical layer aspects*, 3GPP Std. 36.814 v9.0.0, 2010.